Proceedings of Ninth World Conference on Earthquake Engineering
August 2-9, 1988, Tokyo-Kyoto, JAPAN (Vol.VIII)

SI-10

# STUDY ON THE DYNAMIC BEHAVIOR OF MULTISTORY R/C SPACE FRAME STRUCTURES SUBJECTED TO SINUSOIDAL AND EARTHQUAKE BASE MOTIONS

Md. Ali Akbar MOLLICK[1], Takayuki SHIMAZU[1] and Hideo ARAKI[1]

[1]Department of Structural Engineering, Hiroshima University,
Saijo-cho, Higashihiroshima-shi, Japan

## SUMMARY

The objective of this paper is to understand the dynamic behavior of reinforced concrete multistory space frames and to clarify the cooperative effects of slab reinforcement on the increase of beam stiffness and the effects of the simultaneous development into plastic hinge in all beams that frame into the column when subjected to skew earthquake attack. By conducting the shaking table test, various interesting features were obtained regarding the earthquake resistance of reinforced concrete multistory buildings.

## INTRODUCTION

Frame system should be designed to be of beam collapse mechanism to avoid the occurrence of "soft story", but it is difficult to design a frame to be of weak beam-strong column type, due to the insufficient understanding at present stage on cooperative effects of slab reinforcement (Refs.1,2,3) as well as the simultaneous development of plastic hinges in all the beams that frame into the column when subjected to a skew earthquake attack (Ref.4,5). There were experimental works (Refs.2,3,5) with three dimensional specimens to investigate the cooperative effects of slab and biaxial loading effects. However, their focuses were placed on the resistance characteristics of slab-column subassemblages or beam-column subassemblages. Thus shaking table tests were conducted to investigate the overall dynamic behavior of multistory space frame as an assemblage for an important step to the understanding on earthquake resistance of actual buildings.

## EXPERIMENTAL PROGRAM

Test Structures Four test structures of 1/10th scale model, supposed to represent a six-storied single-bay by single-bay multistory space structure, were used in the test. A test structure with dimension is illustrated in Fig.1. The cross sections and reinforcement for members are tabulated in Table 1. Test structures were of beam collapse mechanism in calculation even if cooperative effects of all the slab reinforcement are included. Flexural strength of each member is tabulated in Table 2. The section of columns and their reinforcement were the same over the height of test structures. Test structures were cast horizontally into metal form by the same batch of concrete. River sand of 3.2 mm, maximum size, was used in concrete. The reinforcement used in the fabrication of test structures were of the diameter 1.0, 2.3, 3.2, 4.0 mm with yield strength 4070, 5750, 4480 and 5170 kg/cm$^2$ respectively.

Test Procedure The parameters considered in this study were two, one was the direction of input base motions and the other was the type of input base motions. Two test structures were shaked parallel to long span direction, one of principal axis, to investigate the fundamental dynamic behavior of test structures. The other two test structures were shaked diagonally in order to know the effects of bidirectional input. Setting of test structures on shaking table is shown in Fig.2. Two test structures (SDC-0 and SDC-A) which were parallelly and diagonally shaked were subjected to a series of the sinusoidal base motions of increasing intensity and the other two test structures (SDC-0E and SDC-AE) were subjected to a series of scaled recorded earthquake base motions (1940 El Centro EW). Response spectra of this recorded earthquake base motion at Run 4 are illustrated in Fig.3. Test sequence and mechanical properties of concrete are listed in Table 3. The amplitude of earthquake waves were increased in four steps. Maximum accelerations of both type of base motions at each Run level are listed in Table 4. To measure the relative displacement and absolute acceleration, several displacement transducers and accelerometers were installed at the strategic points of the test structures. During the test a constant gravity load of 240 kg was under application on every floor to get horizontally distributed inertia forces over the height of the test structures.

Table 1 Member Cross section and Reinforcement

| | | |
|---|---|---|
| Column | | b×D=60mm×60mm<br>3-4.0φ Pt=0.79% |
| Beam | Floor Level | b×D=40mm×70mm |
| | R,6 | 2-2.3φ Pt=0.34% |
| | 5,4 | 2-3.2φ Pt=0.66% |
| | 3,2 | 3-3.2φ Pt=0.99% |
| Slab | t=15mm | 1φ @15 in short span<br>1φ @10 in long span |

Hoop and stirrup for members ; 1φ @10

Table 2 Flexural Strength for Members

| Story | Beam Mye* (ton·cm) | Beam Mys** (ton·cm) | Column cMu (ton·cm) | cMu / Mye | cMu / Mys |
|---|---|---|---|---|---|
| 6 | 2634. | 5089. | 9535. | 3.62 | 1.87 |
| 5 | 2634. | 5089. | 9712. | 3.69 | 1.91 |
| 4 | 3960. | 6415. | 9888. | 2.50 | 1.54 |
| 3 | 3960. | 6415. | 10062. | 2.54 | 1.57 |
| 2 | 5927. | 8383. | 10235. | 1.73 | 1.22 |
| 1 | 5927. | 8383. | 10406. | 1.76 | 1.24 |

* without slab ** with slab

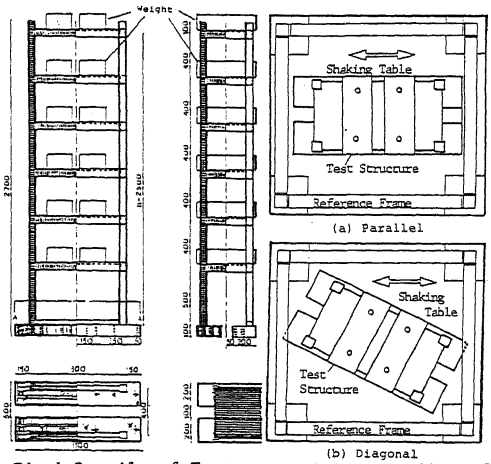


Fig.1 Details of Test Structure

Fig.2 Setting Plan of Test Structure

Table 3 Test Schedule and Mechanical Properties for Concrete

| Test Structure | Base Motion | Direction of Vibration | Concrete Fc | Concrete Ec* |
|---|---|---|---|---|
| SDC-0 | Sine Wave | Parallel | 389. | 2.55 |
| SDC-A | | Diagonal | 415. | 2.48 |
| SDC-0E | Earth-quake Wave | Parallel | 460. | 2.46 |
| SDC-AE | | Diagonal | 418. | 2.49 |

* (×10⁵) at 1/4 Fc unit ; kg/cm²

Table 4 Input Values of Acceleration at Each Run

| Test Structure | Base Motion | Run 1 | Run 2 | Run 3 | Run 4 | Run 5 |
|---|---|---|---|---|---|---|
| SDC-0 | Sine Wave | 38. | 75. | 94. | 125. | 120. |
| SDC-A | | 35. | 80. | 99. | 117. | 130. |
| SDC-0E | Earth-quake Wave | 220. | 348. | 562. | 671. | 688. |
| SDC-AE | | 223. | 311. | 516. | 598. | 688. |

unit ; cm/sec²

Similitude Law Used The similitude law on the test structures used in this test is as follows. The dimension ratio and Young's Modulus Ratio are 1/10 and 1 respectively between the prototype and model. The density ratio modified by adding weight on every floor was 6, instead of 10, taking account of the capacity of the shaking table. From these selections, acceleration ratio and time scale ratio were calculated to be 1.6 instead of 1.0 and 1/4 respectively.

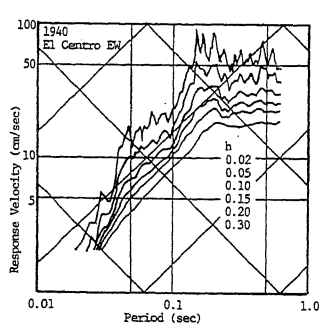


Fig.3 Response Spectra

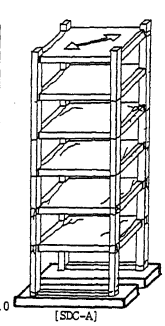


Fig.4 Crack Patterns

## EXPERIMENTAL RESULTS

Crack Patterns Nearly the same crack patterns were observed for all the test structures. For diagonally shaked test structures skew crack lines in slab surface were not observed, different from the static test results reported in (Ref.5), due to the fact that resonance phenomena were observed alternately in both the principal directions in shaking table tests. Flexural cracks at longer beam ends and cracks lines of slab surface along shorter beams were remarkable at each floor. The cracks at shorter beam ends were also observed. This may be due to the torsional effects of slab reinforcement on shorter beams. Fig.4 shows the crack patterns of one of the test structures.

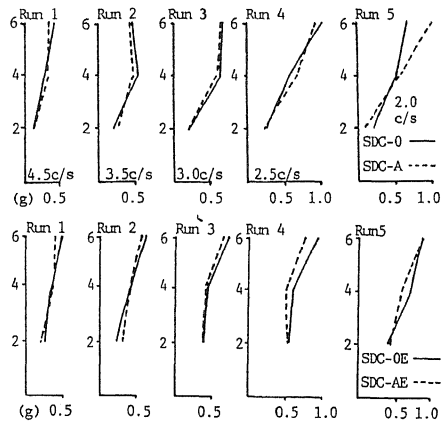


Fig.5(a) Observed Acceleration Distributions

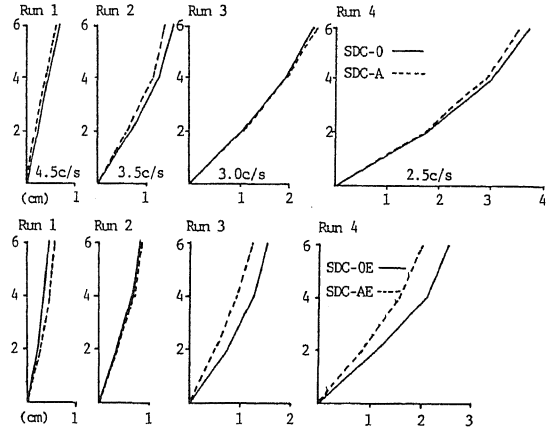


Fig.5(b) Observed Displacement Distributions

Acceleration Distributions The acceleration distributions at maximum base shears at each input level are shown in Fig.5(a). In both cases of parallelly and diagonally shaking tests, accelerations in long span direction were used. Base shear was obtained from: Base Shear $= \sum_{i=1}^{n} mi(\ddot{x}i+\ddot{x}o)$, where, n= total number of story, mi=mass of the ith story, $\ddot{x}i+\ddot{x}o=$ absolute acceleration of the ith story. Acceleration distributions for all the test structures were nearly of the first mode shape at each input level. The higher mode in those distributions for the test structures subjected to earthquake motion (Ref.6) were not observed because the initial fundamental period shown in Table 5 was near the breaking point period which was about 0.2 sec for the response velocity spectra in Fig.3.

Displacement Distributions The lateral displacement distributions at maximum top level displacement at each input level are shown in Fig.5(b). In both cases of parallelly and diagonally shaking tests, the observed values in long span direction were also used. The lateral displacement distributions were inverted-triangular and did not vary throughout the test.

Hysteresis Loops Observed hysteresis loops as the relationships between the base shear and top level displacement at each input level are illustrated in Fig.6. With increase of input amplitude, the features of loops become of slip type (of inverted S type).

## DISCUSSIONS

Outline of Analytical Method The nonlinear frame analysis method (Ref.7) was developed to predict the test results. A test structure was replaced by frame model with imaginary concentrated springs and rigid zone at the ends of the members as shown in Fig.7. An envelope curve (moment-rotation) for each member of the test structure was assumed to be tri-linear as shown in Fig.8. A step-by-step numerical integration procedure is used to solve the equations for static analysis. Distribution of lateral external force was assumed inverted-triangular.

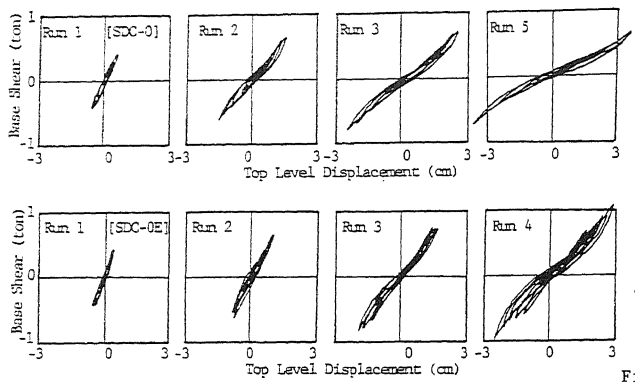


Fig.6 Observed Hysteresis Loops at Each Run Level

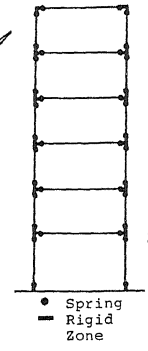


Fig.7 Analytical Model

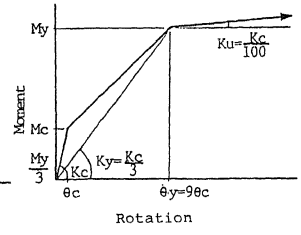


Fig.8 Assumed Envelope Curve

The equations in terms of the relative displacements at the loaded points to the base can be written in an incremental form as follows:

$$\{\Delta P\}+[KH]\{\Delta x\}=\{0\} \qquad (1)$$

$\{\Delta P\}$: incremental external lateral force vector
$[KH]$ : structural stiffness matrix
$\{\Delta x\}$: relative incremental displacement vector

Initial natural periods of test structures were calculated by using the diagonal mass matrix and initial structural stiffness matrix.

Initial Natural Periods and Transitions of Natural Periods The observed and calculated initial periods are shown in Table 5. Observed periods were obtained by small amplitude free vibration tests which were inserted at intervals of each large amplitude input test. Calculated values were obtained ignoring slab effects on beam stiffness. Good agreements are found between the calculated and observed values in both the first and the second modes. Transitions of natural periods along with previously experienced maximum top displacement for all test structures are shown in Fig.9. It is found that natural periods were about 1.5-2.0 times initial periods even at last stage. This may be due to the flexibility of deformation even at final stage.

Table 5 Natural Period

| Test Structure | Observed | | Calculated | |
|---|---|---|---|---|
| | First | Second | First | Second |
| SDC-0 | 0.165 | 0.053 | 0.150 | 0.052 |
| SDC-A | 0.170 | 0.052 | 0.150 | 0.052 |
| SDC-0E | 0.153 | 0.050 | 0.153 | 0.052 |
| SDC-AE | 0.162 | 0.049 | 0.149 | 0.051 |

unit ; sec

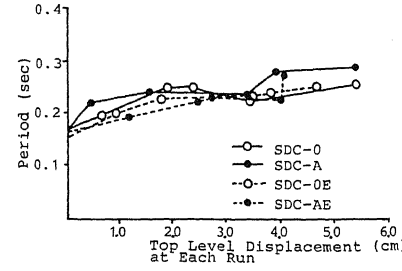


Fig.9 Transitions of Natural Period

Envelope Curves Observed envelope curves of maximum base shear versus top level displacement are plotted in Fig.10. The calculated lines in both the cases of taking account of the effect of all the slab reinforcement (solid line) and ignoring that of all the slab reinforcement (broken line) are also inserted. In comparison between observed and calculated results in sinusoidal base motion tests, it is found that the observed values follow, in the stage from cracking to yielding, the calculated line assuming that all the slab reinforcement is ignored, but approach, at the stage of ultimate strength, the calculated line assuming that all the slab reinforcement is effective. This trend is similar to the results of

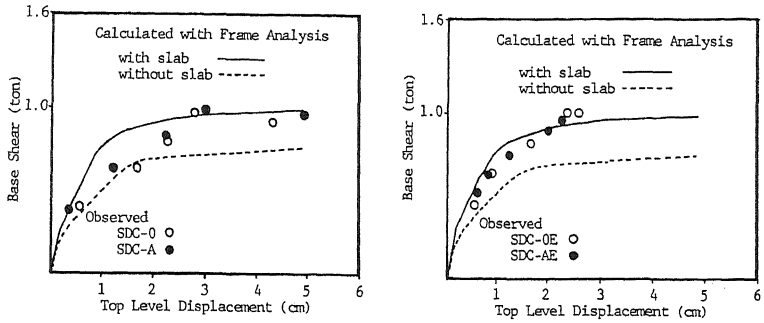


Fig.10 Observed and Calculated Relations between Base Shear and Top Level Displacement

static loading tests reported in Ref.5. On the other hand, the observed values in earthquake base motion tests seem to follow, throughout test, the calculated line assuming that all the slab reinforcement is effective. This result may be due to the effects of higher mode. Remarkable difference between results of both parallelly and diagonally shaked test structures were not observed.

Displacement Time History and Orbital Plots The observed and calculated displacement time histories and orbital plots at top mass center of test structures for the diagonally shaked test structures subjected to sinusoidal base motion are illustrated in Fig.11. For the diagonally shaked test structures resonance phenomena can be observed not in diagonal direction but alternately in principal axis. To understand these phenomena, dynamic response analysis was conducted by using the simplified analytical method (Ref.8). Test structures were assumed to be two degrees of freedom system with the equivalent mass and the equivalent height shown in Fig.12. Bilinear envelope curves for this system were obtained by simplifying the envelope curves calculated by the frame analysis assuming that all the slab reinforcement were effective. The restoring force characteristics were assumed as origin oriented. Results of analysis for the diagonally shaked test structure subjected to sinusoidal base motion are shown in Fig.11. Good agreements are found between the calculated and observed time histories and orbital plots. The same results were obtained for the test structures subjected to earthquake base motions, by using the two degrees of freedom system.

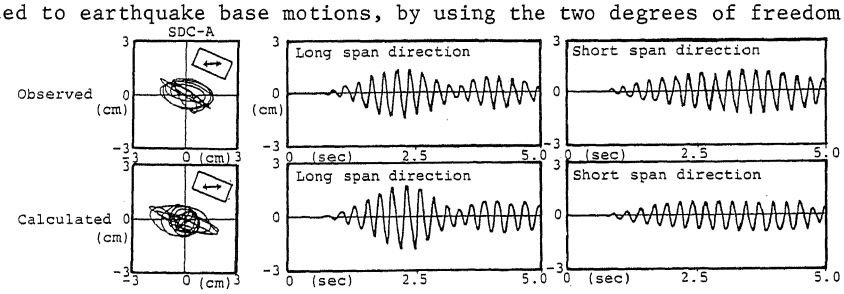


Fig.11 Observed and Calculated Displacement Time Histories and Orbital Plots of Mass Center

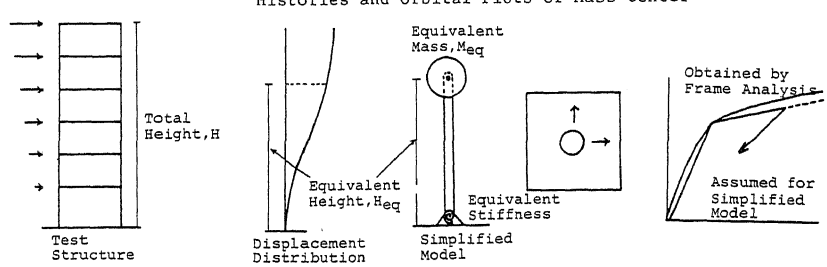


Fig.12 Assumed Analytical Model for Simplified Method

Responses The relation between both the base shear and top level displacement and input levels are shown in Fig.13. Base shear was divided by the calculated lateral strength of the test structure Pcu, obtained by the virtual work method assuming that all the slab reinforcement are effective and that the distributions of external forces are inverted-triangular. Displacement are normalized with deflection angle R. Base shears are also normalized by dividing with Pcu/M. Thus the ratio of both axis become magnification factor:

$$\text{Magnification Factor} = \sum_{i=1}^{n} mi(\ddot{x}i+\ddot{x}o) \;/(M\cdot\ddot{x}o) = (\text{Base Shear}/Pcu)/(M\cdot\ddot{x}o/Pcu) \qquad (2)$$

Pcu : Lateral strength of structure
M : total mass of structure

Fig.13 shows that the magnification factors of the test structures subjected to sinusoidal base motion are 7-8 at the first stage, and become about 5 at the last stage. It is also found that sinusoidal waves power are much stronger than earthquake waves power in which magnification factors are 2-3 at most. The results of single story space structures in (Ref.9) are also plotted in this figure. S and E represent the case of sinusoidal and earthquake waves respectively. The difference between two types of test structures is considered due to their difference in overall proportion related to flexibility of deformation.

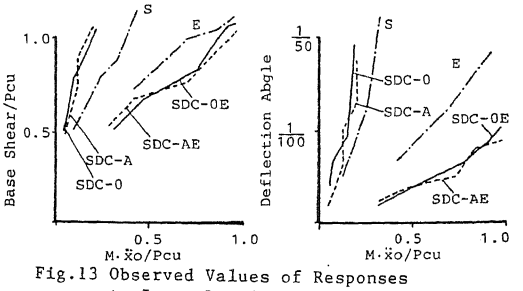

Fig.13 Observed Values of Responses to Input Levels

## CONCLUSIONS

This paper presents the shaking table tests conducted to investigate the dynamic behavior of reinforced concrete multistory space frame structures, when subjected to strong base motions. Based on the experimental and analytical results, the following statements can be made. An important step to the understanding on earthquake resistance of actual buildings was made with the focuses on the cooperative effects of slab and biaxial loading effects.

## ACKNOWLEDGEMENTS

The authors would like to express their thanks to C. Fujita and Y. Monji, the graduate students of the Hiroshima University for their cooperation. The experimental work had been performed by using the Earthquake Simulator of Chugoku Electric Co. Ltd.

## REFERENCES

1. Yoshimura, M. and Tsubosaki, H.,"U.S.-Japan Cooperative Research on RC Full-Scale Building Test (Part 6 Ultimate Moment-Resisting Capacity),"The Proc. of the Eighth World Conference on Earthquake Engineering, Vol.6, pp.635-642.
2. Morrison, G. Denby, Hirasawa, I. and Sozen, Mete A.,"Lateral-Load Tests of R/C Slab-Column Connections," The Proc. of ASCE,Vol.109, ST11, Nov.,1983, pp.2698-2714.
3. Morrison, G. Denby,"Dynamic Lateral Load tests of R/C Column-Slabs,"The Proc. of ASCE,Vol.111, ST3, March, 1985, pp.685-698.
4. Park, P. and Paulay, T.,"Reinforced Concrete Structures," John Willey & Sons, 1975 p.603.
5. Suzuki, N., Otani, S.and Kobayashi, Y.,"Three-Dimension Beam-Column Subassemlage under Bidirectional Earthquake Loading,"The Proc. of the Eighth World Conference on Earthquake Engineering, 1984, Vol.6, pp.453-460.
6. Araki, H. and Shimazu, T.,"Fundamental Study on the Dynamic behavior of RC Multistory Plane Frames,"Journal of Structural Engineering, Vol.33B, March,1987, pp.145-154.
7. Giberson, M. F.,"Two Nonlinear Beams with Definitions of R.C. Buildings," The Proc. of ASCE,ST2, Vol.95, Feb. 1969, pp.137-157.
8. Saiidi, M. and Sozen, M.A.,"Simple Nonlinear Seismic Analysis of RC Structures " The Proc. of ASCE, ST5, May, 1981,pp.937-951.
9. Shimazu, T. and Araki, H., "Fundamental Study on Dynamic Torsional Responses of RC Space Structure,"Journal of Structural Engineering, Vol.32B, March,1986, pp.159-170.